crystals

MDPI

Article

Mechanical Performance and Deformation Behavior of CoCrNi Medium-Entropy Alloy at the Atomic Scale

ZF Liu [1,†], N Tian [2,†], YG Tong [2,*], YL Hu [2], DY Deng [2], MJ Zhang [2], ZH Cai [3] and J Liu [3,*]

[1] College of Aerospace Science and Engineering, National University of Defense Technology, Changsha 410114, China; liuzhuofeng@nudt.edu.cn
[2] College of Automobile and Mechanical Engineering, Changsha University of Science and Technology, Changsha 410114, China; 18711175611@163.com (N.T.); ylh@163.com (Y.H.); ddy@163.com (D.D.); zmj@163.com (M.Z.)
[3] National Engineering Research Center for Mechanical Product Remanufacturing, Army Academy of Armored Forces, Beijing 100072, China; czh@163.com
* Correspondence: tongyonggang_csust@163.com (Y.T.); xbdliu5899@163.com (J.L.)
† These authors contributed equally to this work.

Abstract: CoCrNi medium-entropy alloy has superior cryogenic properties with simultaneous growth of strength and plasticity at low temperatures. In order to observe the microstructure and deformation behavior of the alloy at the atomic scale, its mechanical properties and deformation mechanism at different temperatures and strain rates were investigated using molecular dynamics. It is indicated that the alloy's strength was enhanced at low temperatures and high strain rates due to the production of high dislocation density. The introduction of grain boundaries significantly decreased the dislocation density during the alloy's deformation and correspondingly reduced the crystal strength. However, the introduction of twin boundaries in polycrystalline grains obviously enhanced the strength of the polycrystal, especially at the twin boundary spacing of 3.08 nm. The strength's enhancement was attributed to the increasing dislocation density produced by the interaction between twin boundaries and dislocations during deformation.

Keywords: medium-entropy alloy; twin boundary; mechanical properties; molecular dynamics

Citation: Liu, Z.; Tian, N.; Tong, Y.; Hu, Y.; Deng, D.; Zhang, M.; Cai, Z.; Liu, J. Mechanical Performance and Deformation Behavior of CoCrNi Medium-Entropy Alloy at the Atomic Scale. *Crystals* **2022**, *12*, 753. https://doi.org/10.3390/cryst12060753

Academic Editors: Yang Zhang and Yuqiang Chen

Received: 22 April 2022
Accepted: 17 May 2022
Published: 24 May 2022

1. Introduction

Medium-entropy alloys (MEAs) are a new class of metallic structural materials with great potential for application, which are composed of multiple principal elements in equal or near equal molar ratio distributed on the topologically ordered crystallographic lattices with a high chemical disorder [1,2]. Currently, MEAs are attracting extensive research interest, particularly the face-centered cubic (FCC) phase CrCoNi MEA, which has been found to display excellent mechanical properties, including high fracture toughness and high strength [3,4]. Compared to room temperature, the strength, ductility, and toughness of the CoCrNi alloy increased simultaneously at cryogenic temperatures, reaching strength of more than 1.3 GPa and failure strains up to 90% [4].

Previous studies have shown that the FCC-phase CoCrNi MEAs exhibit excellent mechanical properties due to the relatively low stacking fault energy (SFE) value (18 mJ/m^2) [5,6]. The lower SFE makes it easier to produce more nanotwins during deformation, resulting in better mechanical properties, especially at cryogenic temperatures [6]. At present, studies of SFE, dislocation, and nanotwins in MEAs are mainly conducted on the basis of experiments. Woo et al. [7] investigated dislocation density, twin fault probability, and SFE of CoCrNi-based MEAs deformed at different temperatures by using in-situ neutron diffraction and peaks profile analysis methods. Cao et al. [8] investigated plastic deformation mechanisms in FCC materials with low SFE by using transmission electron microscopy. However, experimental investigations can hardly track the microstructure changes during deformation

in real time. Molecular dynamics (MDs) simulations are an effective tool to investigate the relationship between microstructure and properties at the atomic scale [9]. Atomic simulations have been demonstrated to provide real-time and atomic-scale monitoring of the deformation processes, such as nucleation and movement of dislocation [10–12]. Therefore, in the present study, we employed MDs to study the microstructure and mechanical properties of CoCrNi single crystals (SCs) at different temperatures and strain rates. Then, we inserted grain boundaries (GBs) and twin boundaries (TBs) to further study the deformation mechanism of polycrystals. The effects of GBs and TBs on the mechanical properties of MEAs were revealed by comparative analysis, which will help to design strong and highly ductile nanotwinned MEAs.

2. Simulation Methods

The atomic-scale SC model is shown in Figure 1a. The SC was oriented with its <100>, <010>, and <001> aligned respectively with the x-, y-, and z-axes. The average lattice parameter of the CoCrNi alloy is 3.559 Å, and the cohesive energy obtained at this point is -4.32 eV/atom. In order to study the effect of crystal orientation on mechanical properties, another model with different crystal orientations was established. This sample was oriented with its <001>, <1$\bar{1}$0>, and <110> aligned with the x-, y-, and z-axes. For the polycrystalline model, eight randomly oriented grains were created using the Voronoi construction method [13]. The obtained polycrystalline structure is shown in Figure 1b. For polycrystals with nanotwins, single crystals with certain twin boundary spacing (λ = 1.85, 2.47, 3.08, 3.70, and 4.32 nm) were constructed first, and then polycrystals with nanotwins were constructed through the Voronoi construction method, as shown in Figure 1c. The sizes of MEA samples were 106.77 × 106.77 × 106.77 Å in X, Y, and Z directions (~108,000 atoms). Three types of atoms were equimolarly randomly distributed. Periodic boundary conditions were employed in all three directions. The timestep was always 1fs in the simulation. The conjugate gradient algorithm was used to minimize the energy of all samples. The energy tolerance and force tolerance were 10^{-12} and 10^{-12}, respectively. Various temperatures (77, 300, 500, and 800 K) were calculated. For every temperature, the samples were relaxed by the Nose–Hoover isobaric-isothermal (NPT) ensemble for 100 ps. After the balancing process, the samples were deformed at a strain rate of 1×10^8 to 1×10^{10} s^{-1} along the Z direction.

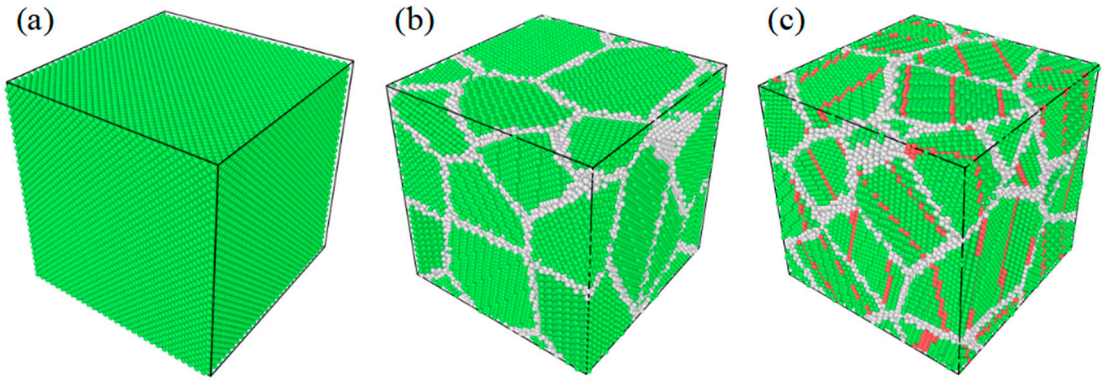

Figure 1. CoCrNi MEA model of FCC phase simulated by MD. (**a**) SC, (**b**) polycrystal, (**c**) polycrystal with TB spacing λ = 1.83 nm. FCC atoms are colored green, GBs are colored white, TBs are colored red.

All models were constructed by Atomsk software. Molecular dynamics calculations were performed using the Large-Scale Atomic/Molecular Massively Parallel Simulator (LAMMPS) [14]. The atomic interaction in CoCrNi MEA adopted the embedded atom method (EAM) potential developed by Li et al., which has been used in some MD studies involving nucleation and motion of dislocation [15]. The Ovito software was used for visualization and statistical analysis of structures [16]. Common neighbor analysis (CNA)

and dislocation extraction algorithm (DXA) were used to identify lattice structures and dislocations [17–19].

3. Results and Discussion

3.1. Single Crystalline MEA

3.1.1. Effect of Temperature

The stress-strain curves of CoCrNi MEA under tension and compression at different temperatures are shown in Figure 2. With increasing the temperature from 77 to 800 K, the tensile strength along the <110> direction decreases from 13.75 to 6.60 GPa (Table 1). Different from the linear elastic deformation region that occurs in the <001> direction, the stress of the samples grows nonlinearly throughout the elastic deformation region when tensioned in the <110> direction, as shown in Figure 2a. In addition, the tensile strength of the samples along the <110> direction decreases significantly. This is presumably due to the anisotropy of materials, where the <110> direction has a higher density of atomic arrangement and is more prone to slip deformation. In this study, compression of CoCrNi at different temperatures was also calculated. Similar to the tensile strength, the compressive strength decreases with increasing temperatures, as shown in Table 1 and Figure 2b.

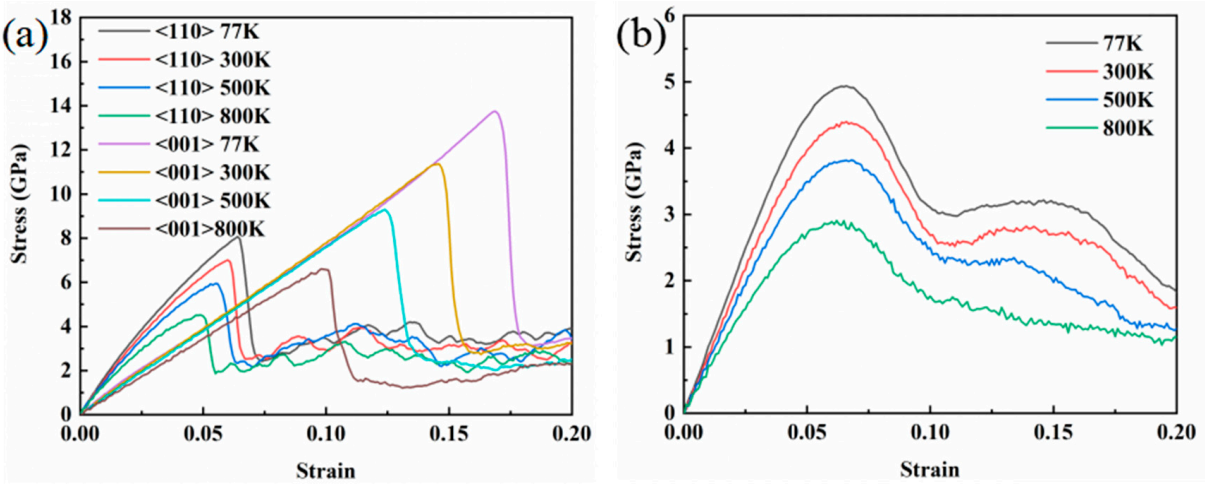

Figure 2. (**a**) Tensile stress-strain curves in <001> and <110> directions at different temperatures, (**b**) compressive stress-strain curves in <001> direction at different temperatures.

Table 1. Tensile and compressive strength of CoCrNi at different temperatures.

Temperatures	Tensile Strength (GPa)		Compressive Strength (GPa)
	<001>	<110>	<001>
77 K	13.75	8.07	4.93
300 K	11.36	7.01	4.40
500 K	9.30	5.95	3.81
800 K	6.60	4.52	2.91

In order to study the effect of temperature on the mechanical properties and deformation behavior, the stress and structural evolution during compression at different temperatures were investigated. As shown in Figure 3, FCC atoms dominate during the elastic deformation. The body-centered cubic (BCC) atoms emerge with the strain increased, leading to a decrease in the slope of the nonlinear elastic region. After reaching the maximum value, the stress starts to drop, at which time the hexagonal close-packed (HCP) atoms rapidly generate and expand from the BCC atomic aggregation. The massive formation and accumulation of dislocations, mainly Shockley dislocations (the green line in Figure 4 represents the Shockley dislocation) slow down the stress drop. Compared with the short

dislocations generated at high temperatures, the long and twisted dislocations generated at low temperatures have a greater inhibitory effect on the stress drop, which results in a faster stress drop at high temperatures than at low temperatures, as shown in Figure 4.

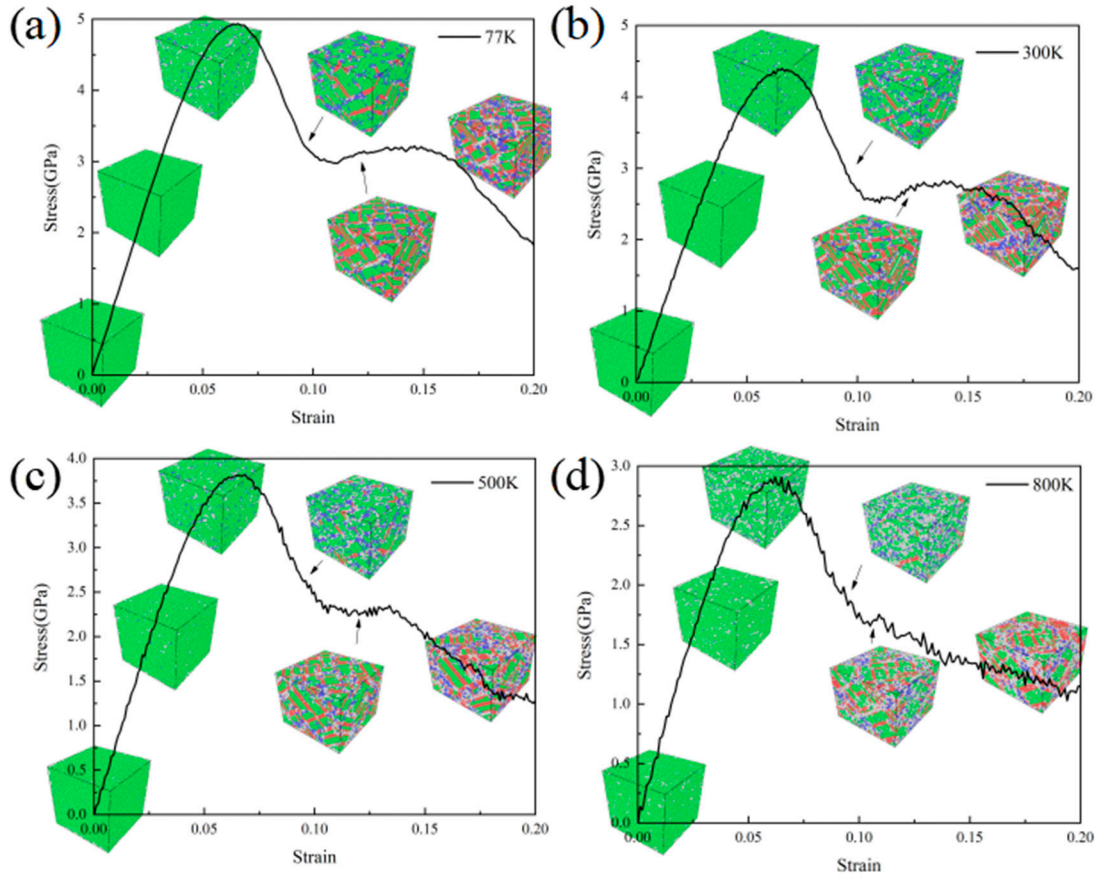

Figure 3. Stress and structural evolution of CoCrNi SCs at 77 K (**a**), 300 K (**b**), 500 K (**c**), and 800 K (**d**). Green, blue, and red represent the atoms of FCC, BCC, and HCP structures, respectively. The arrows indicate the microstructure of the alloy when the strain is 0%, 3%, 6%, 9%, 12% and 15%.

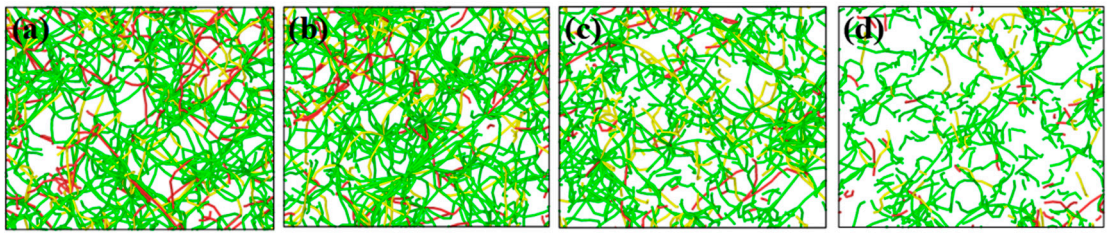

Figure 4. Dislocation distribution at 77 K (**a**), 300 K (**b**), 500 K (**c**), and 800 K (**d**) under the same strain rate.

3.1.2. Effect of Strain Rate

The mechanical properties of CoCrNi MEA at different strain rates of 1×10^8, 1×10^9, and 1×10^{10} s^{-1} are shown in Figure 5 and Table 2. As the strain rate increases, the elastic modulus is constant, while the maximum stress increases significantly. As shown in Figure 5a, the maximum tensile stress along the <110> direction is lower than that in the <001> direction because the higher density of atomic arrangement in the <110> direction makes slip deformation easier. To further analyze the mechanical and structural responses at different strain rates during the compression process, the stress and structural evolution at strain rates of 1×10^8, 1×10^9, and 1×10^{10} s^{-1} were tracked. Until the strain reaches

~5%, the atoms maintain the FCC structure and the stress increases linearly with the increase of strain. After the strain reaches ~5%, some of the atoms deviate from their equilibrium positions and rearrange themselves into BCC structure with lower coordination number, leading to a decrease in the slope of the nonlinear elastic region. At the beginning of plastic deformation at strain rates of 1×10^8 s^{-1}, the HCP structure rapidly generates and expands, resulting in a sharp decrease in stress, as shown in Figure 6a. However, after the plastic deformation begins at strain rates of 1×10^{10} s^{-1}, many small stacking faults (SFs) are formed, which intersect each other and eventually form a dense three-dimensional network of SFs, as shown in Figure 6b. The network hinders the further growth of small dislocation loop and thus, the stress drop is delayed.

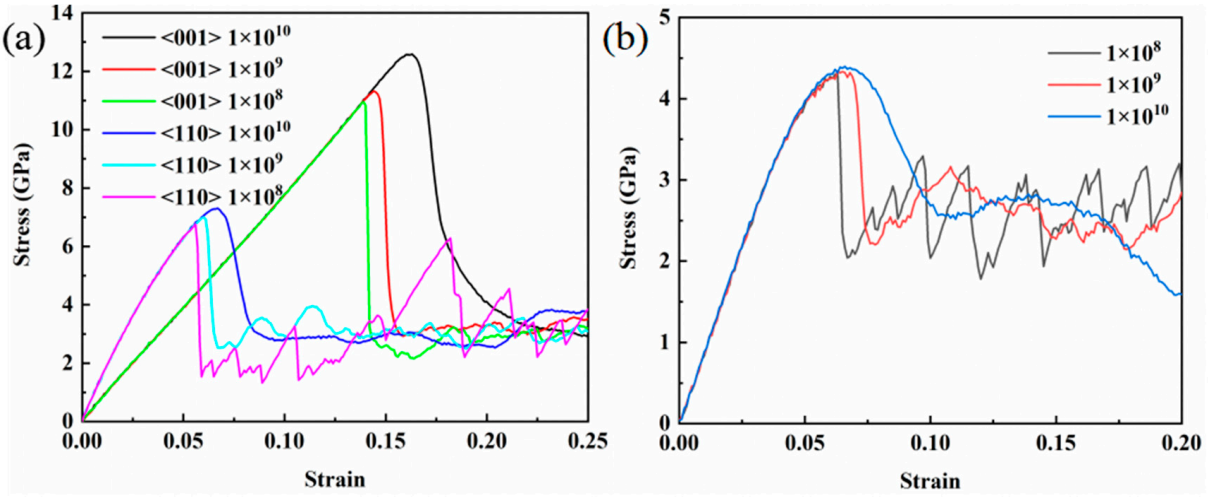

Figure 5. (**a**) Tensile stress-strain curves in direction <001> and <110> at different rates, (**b**) compressive stress-strain curves in direction <001> at different rates.

Table 2. Tensile and compressive strength of CoCrNi at different strain rates.

Strain Rates	Tensile Strength (GPa)		Compressive Strength (GPa)
	<001>	<110>	<001>
1×10^8 s^{-1}	10.96	6.76	4.27
1×10^9 s^{-1}	11.32	7.01	4.34
1×10^{10} s^{-1}	12.59	7.30	4.38

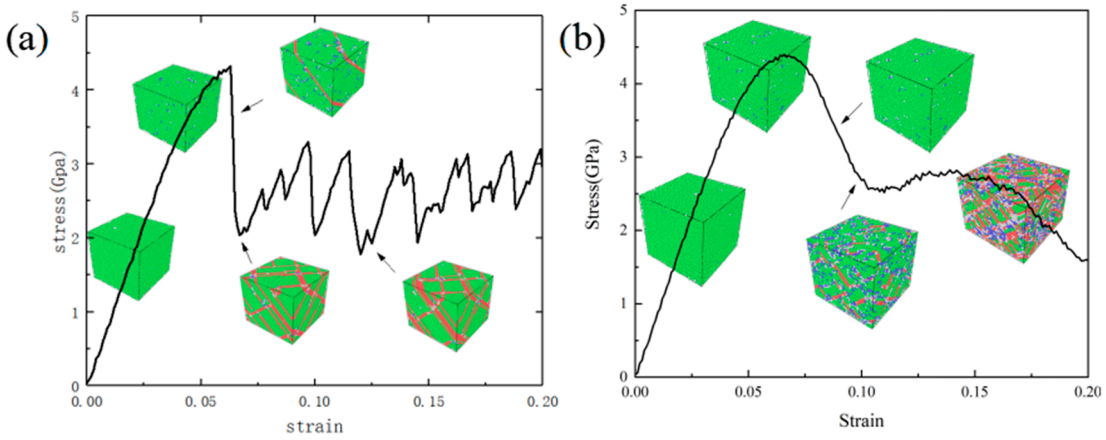

Figure 6. Stress and structural evolution of CoCrNi SCs at strain rates of 1×10^8 s^{-1} (**a**) and 1×10^{10} s^{-1} (**b**). Green, blue, and red represent the atoms of FCC, BCC, and HCP structures, respectively.

3.2. Polycrystalline MEA

Ideal SCs of a certain size are extremely rare in nature. The alloys in practical applications are usually polycrystals. Therefore, we further discussed the mechanical behavior and deformation mechanism of CoCrNi polycrystals.

Figure 7 shows the structural evolution of CoCrNi polycrystals at different strains when stretched at 77 K. During the deformation, SFs and nanotwins generate and expand. With the increase of strain, GBs slip and the proportion of atoms in the disordered state at the GBs increases. In order to consider the effect of temperature on the mechanical properties and deformation behavior of polycrystals, the stress-strain curves at different temperatures are shown in Figure 8. Similar to the effect of temperature on mechanical properties at SCs, the tensile strength and modulus of elasticity increase with decreasing temperature. By comparing the structure and dislocation distribution after tension at different temperatures, it can be found that the deformation at low temperature is dominated by dislocation movement, and the deformation at high temperature is dominated by GBs slip, as shown in Figure 9.

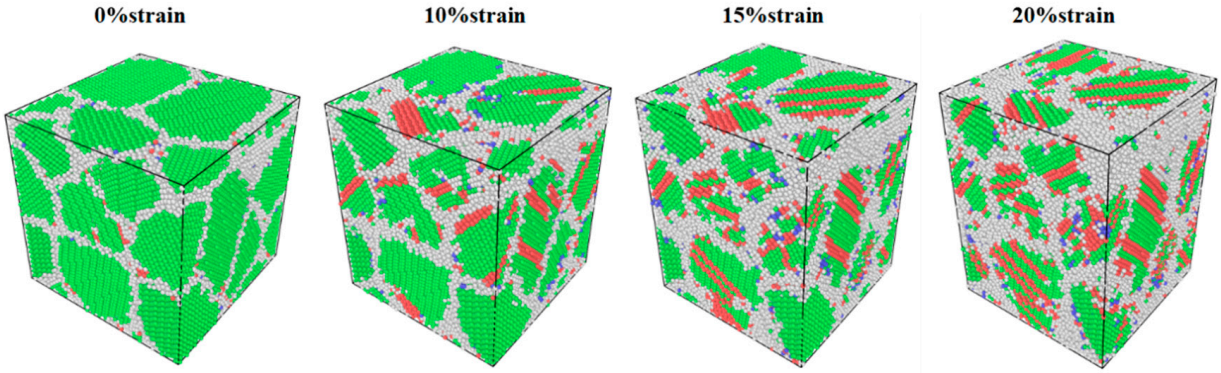

Figure 7. Structural evolution of CoCrNi polycrystals at different strains.

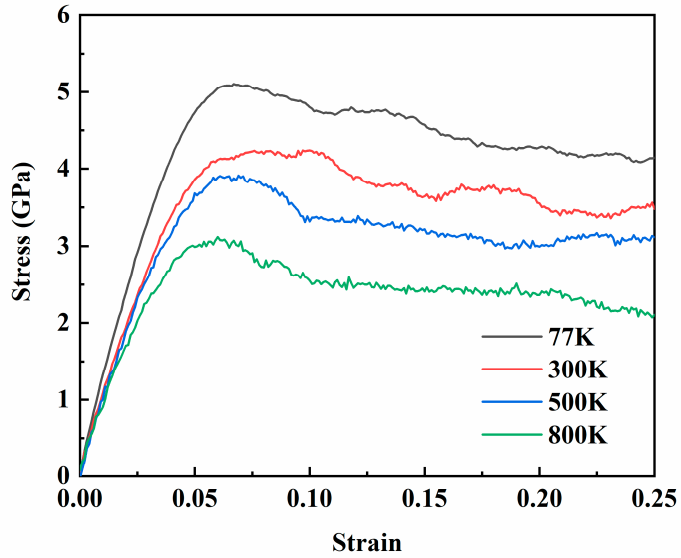

Figure 8. Stress-strain curves of CoCrNi polycrystals at different temperatures.

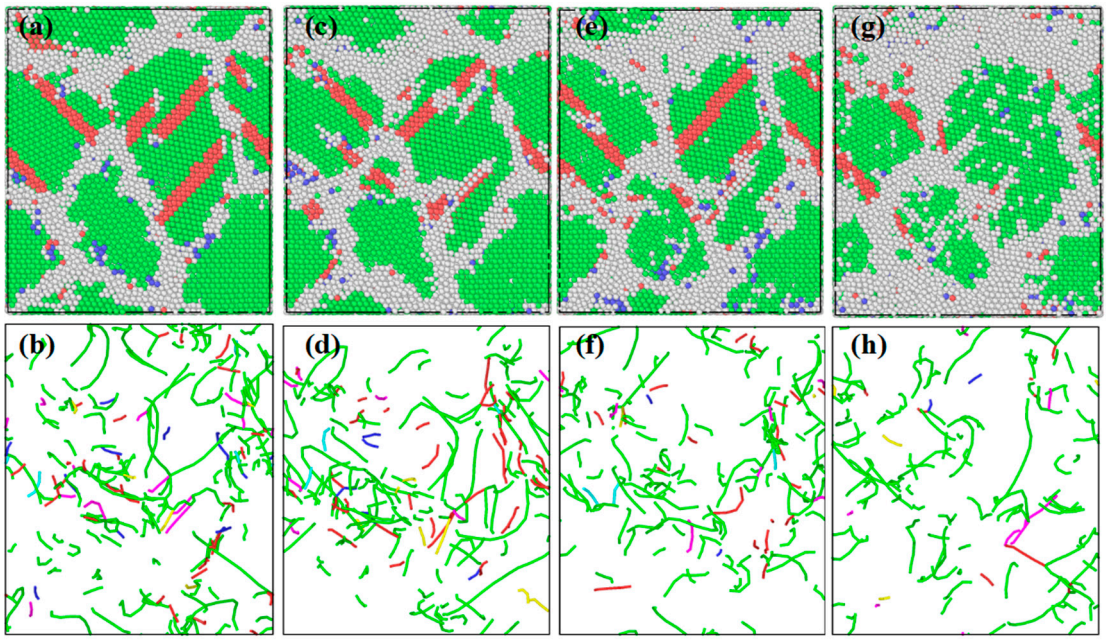

Figure 9. Structure and dislocations of CoCrNi polycrystals at 10% strain at 77 K (**a**,**b**), 300 K (**c**,**d**), 500 K (**e**,**f**), and 800 K (**g**,**h**).

3.3. Nanotwinned MEA

As can be seen from the work on SCs and polycrystals, a large number of dislocations and nanotwins are generated during the deformation process. The effect of dislocations on the mechanical properties and deformation behavior is obvious. However, the role of nanotwins is not reflected. Therefore, in this part, nanotwins with different spacing (λ) were introduced in the initial polycrystalline model to investigate the effect of TBs on mechanical performance of CoCrNi MEA.

3.3.1. Effect of Strain Rate

In this study, the effect of TB spacing on the mechanical properties was investigated using polycrystals with nanotwins as the research object. Figure 10a shows the stress-strain curves of samples with different TB spacing at 300 K. The stress of all stress-strain curves decreased after reaching maximum stress, which was commonly found in MD simulations and attributed to the nucleation of dislocations [20,21]. As shown in Figure 10b, with the increase of λ, the maximum stress increases firstly and then decreases after λ = 3.08 nm.

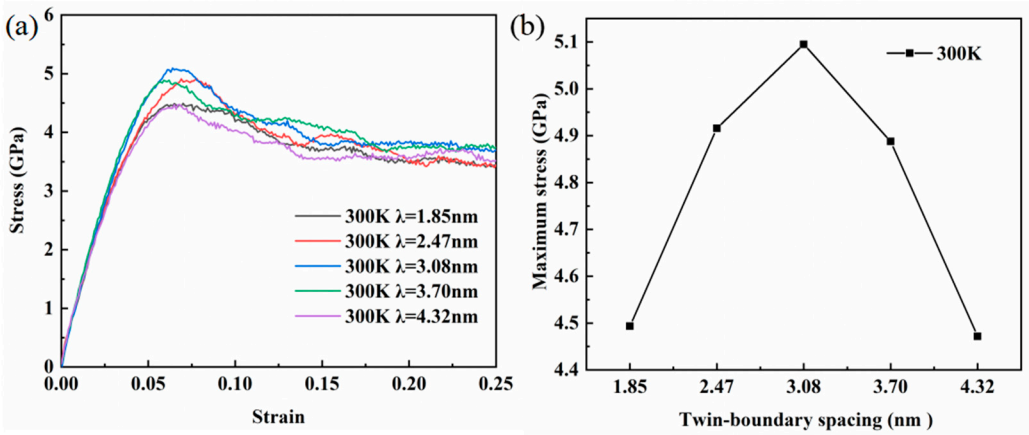

Figure 10. (**a**) Stress-strain curves of samples with different λ (from 1.85 to 4.32 nm) at 300 K, (**b**) maximum stress at different λ at 300 K.

In order to further reveal the effect of λ on mechanical properties of CoCrNi MEAs, the structures and dislocations of samples with different λ at 10% strain are shown in Figure 11d–i. For comparison, the initial structures with different λ are also displayed, as shown in Figure 11a–c. When λ = 1.85 nm, partial Shockley dislocations are perpendicular to and interacting with TBs. When λ = 3.08 nm, the dislocations are no longer perpendicular to the TBs. At this time, a large number of dislocations are entangled with each other, resulting in an increase in the density of dislocations, which improves the mechanical properties of the alloy. When λ = 4.32 nm, the interaction among TBs weakens and the dislocations reduce. Thus, the ability to delay stress drop is reduced.

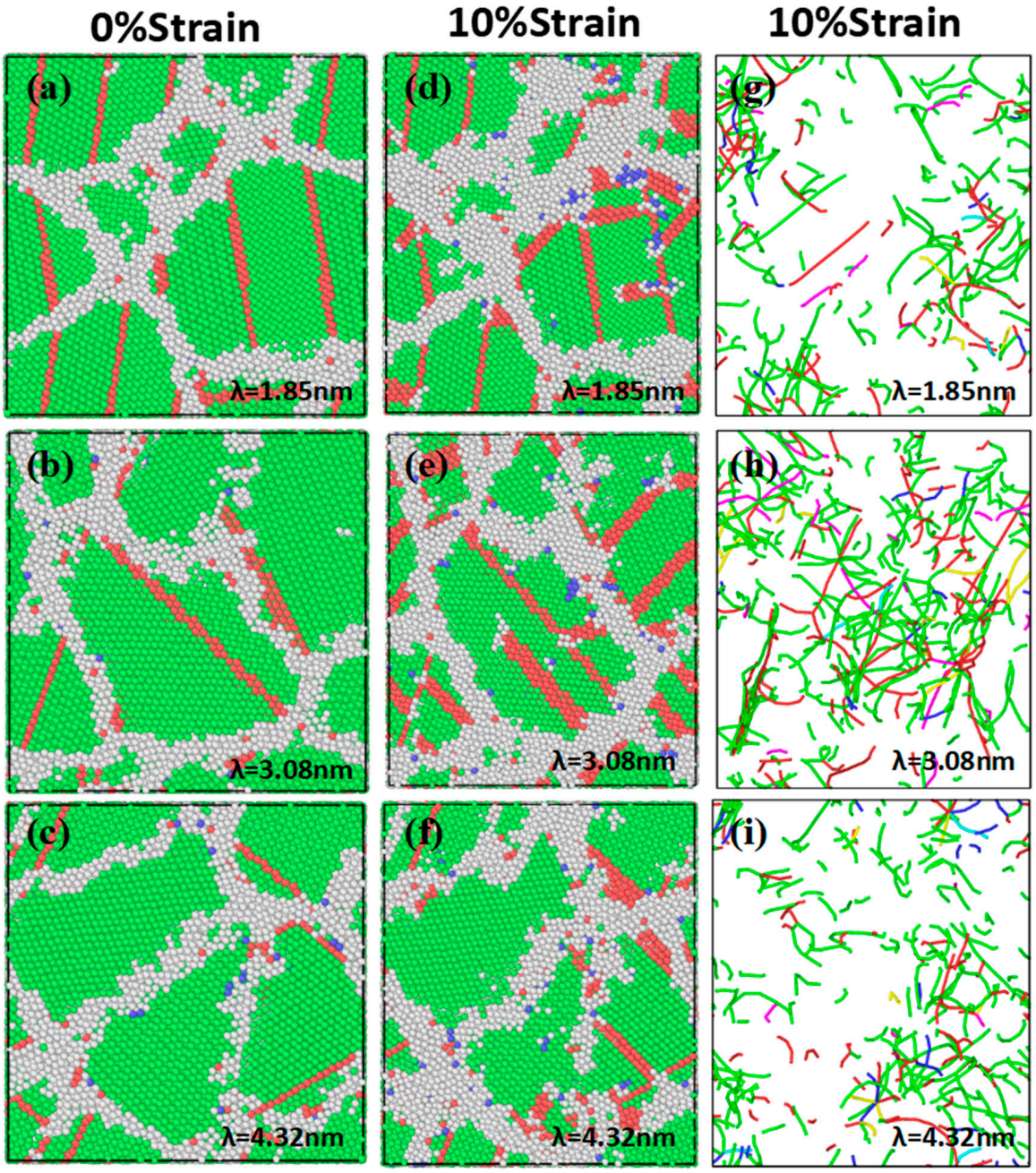

Figure 11. Initial structures at 300 K with TB spacing of (**a**) 1.85 nm, (**b**) 3.08 nm, and (**c**) 4.32 nm, structure of the samples at the strain of 10% with TB spacing of (**d**) 1.85 nm, (**e**) 3.08 nm, and (**f**) 4.32 nm, and dislocations of the samples at the strain of 10% with TB spacing of (**g**) 1.85 nm, (**h**) 3.08 nm, and (**i**) 4.32 nm.

3.3.2. Effect of Temperature

In order to investigate the effect of temperature on the mechanical properties of polycrystals with nanotwins, tensile tests at 77, 300, 500, and 800 K were conducted. The stress-strain curves of samples at different temperatures are shown in Figure 12a–d. As the temperature increases, the tensile strength decreases. Similar to the previous trend exhibited at 300 K, the trend of the maximum stress of the samples at other temperatures increases and then decreases with decreasing λ, reaching a maximum at λ = 3.08 nm (Figure 12e). To further understand the effect of temperature on the mechanical properties of polycrystals with nanotwins, the deformation mechanism and dislocation movement of the alloy at different temperatures were studied. The structure and dislocations at different temperatures are shown in Figure 13. At high temperatures, the GBs slip is obvious. The proportion of disordered atoms at the GB increases, and the dislocation density is small. At low temperatures, dislocations move more slowly, which may lead to dislocation entanglement, resulting in higher dislocation density. The high dislocation density delays the stress drop and enhances the mechanical properties of the alloy. With the decrease of temperature, the deformation mechanism dominated by the GBs slip changes to that dominated by dislocation slip.

In order to reveal the effects of GBs and TBs on the mechanical properties of CoCrNi MEAs, we compared the tensile results of SCs, polycrystals, and polycrystals with nanotwins under the same conditions. As shown in Figure 12f, SCs have the highest strength, followed by polycrystals with nanotwins and polycrystals without nanotwins. Polycrystals have different crystal orientations, complicated GBs, and many lattice defects; therefore, the polycrystals have the smaller strength compared with SCs. Then, comparing Figures 9 and 13, we found that the introduction of nanotwins increased the dislocation density of the polycrystals due to the interaction between the nanoscale TBs and dislocations, which further improves the strength of polycrystals. Liang et al. [22] investigated the deformation mechanism of the CoCrNi alloy with a high density of annealing twins by in situ transmission electron microscopy and also found that TBs not only strengthen the material by hindering the motion of dislocations but also act as a dislocation source to produce slip bands. In addition, Deng et al. [23] also tailored mechanical properties of a CoCrNi medium-entropy alloy by controlling nanotwin-HCP lamellae and annealing twins. Therefore, TBs significantly affect the mechanical properties, and introducing appropriate TB spacing will help to realize the strengthening of the alloy.

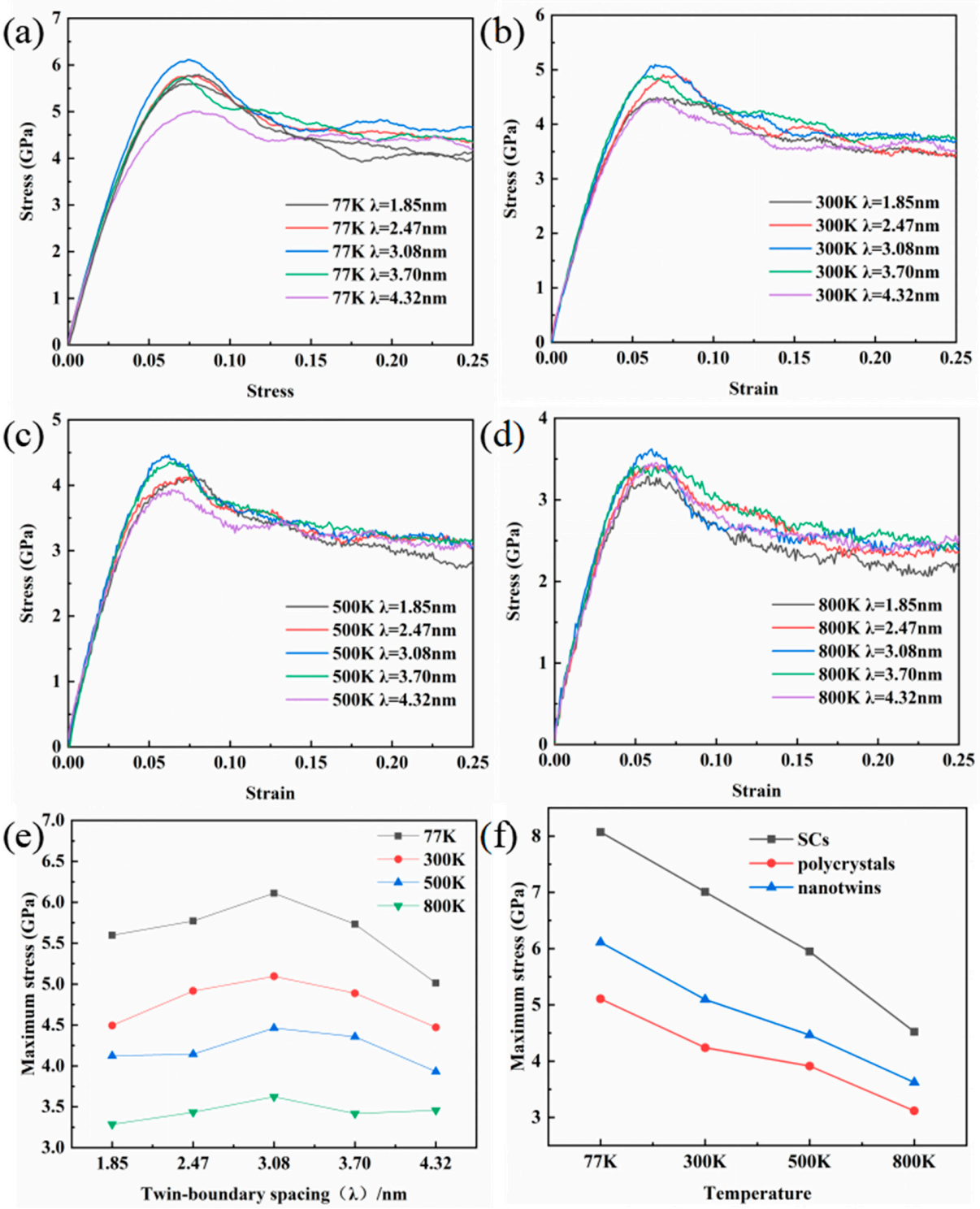

Figure 12. Stress-strain curves of samples with different TB spacing at 77 K (**a**), 300 K (**b**), 500 K (**c**) and 800 K (**d**), (**e**) maximum stress for samples with different spacing at different temperatures, (**f**) maximum stresses of SCs, polycrystals, polycrystals with nanotwins at different temperatures.

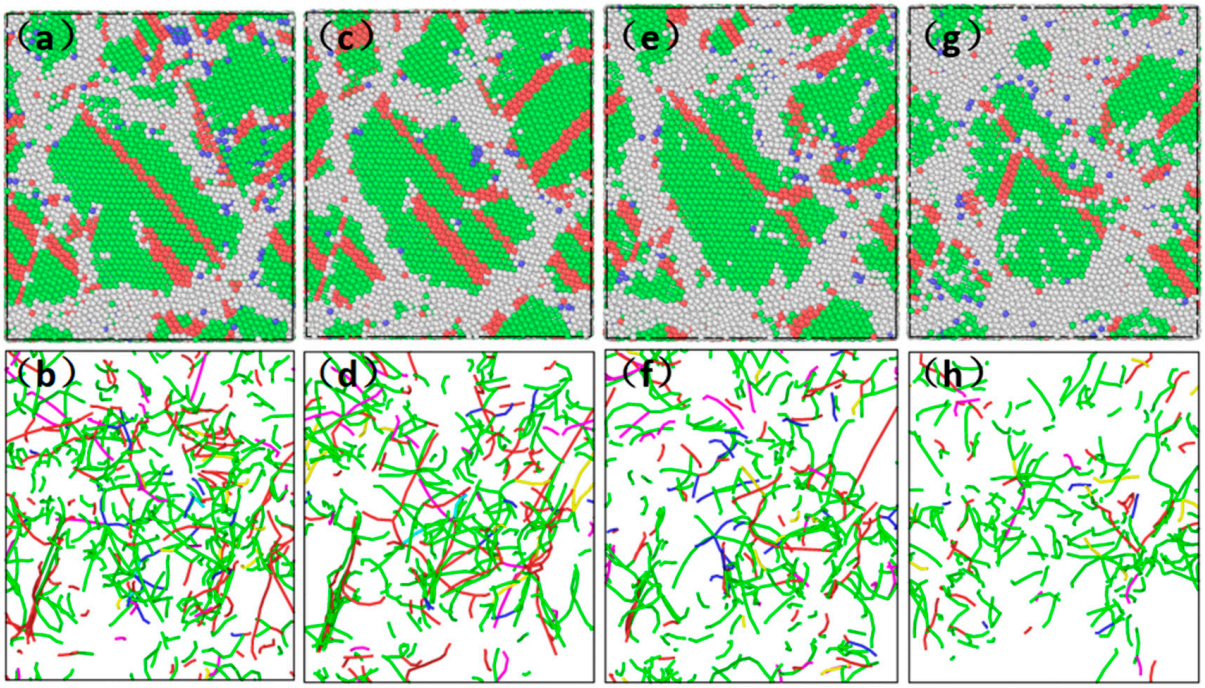

Figure 13. Structure and dislocations of CoCrNi samples with λ = 3.08 nm at 10% strain at 77 K (**a**,**b**), 300 K (**c**,**d**), 500 K (**e**,**f**), and 800 K (**g**,**h**).

4. Conclusions

In this study, the effects of temperature, strain rate, and TB spacing on the mechanical properties and deformation mechanisms of CoCrNi MEAs were investigated by MD simulations. The following conclusions were obtained through a series of comparative analyses:

(1) The strength of CoCrNi increases with the decrease of temperature and the increase of strain rate because the dislocations in the crystal are more intensive at low temperature and high strain rate;

(2) The introduction of defects such as GBs and nanotwins can greatly reduce the strength of SCs;

(3) The presence of TBs can effectively enhance the strength of the polycrystals. The strength increases with the increase of TB spacing when λ is lower than 3.08 nm, and decreases with the increase of spacing when it is higher than 3.08 nm.

Author Contributions: N.T., Z.L. and Y.T. contributed the central idea, calculations, data analysis and drafting of the paper. Y.H., D.D., M.Z., Z.C. and J.L. contributed to refining the ideas, carrying out additional analyses and finalizing this paper. All authors have read and agreed to the published version of the manuscript.

Funding: This research was funded by National Natural Science Foundation of China (No. 92166105 and 52005053), High-Tech Industry Science and Technology Innovation Leading Program of Hunan Province (No.2020GK2085), Hunan Youth Science and Technology Innovation Talent Project (2021RC3096), and Open fund of Key Laboratory of New Processing Technology for Nonferrous Metal & Materials Ministry of Education (No. 20KF-24).

Institutional Review Board Statement: Not applicable.

Informed Consent Statement: Not applicable.

Data Availability Statement: Not applicable.

Conflicts of Interest: The authors declare that they have no known competing financial interest or personal relationships that could have appeared to influence the work reported in this paper.

References

1. Cao, F.-H.; Wang, Y.-J.; Dai, L.-H. Novel atomic-scale mechanism of incipientplasticity in a chemically complex CrCoNi medium-entropy alloy associated with inhomogeneity in local chemical environment. *Acta Mater.* **2020**, *194*, 283–294. [CrossRef]
2. Jian, W.-R.; Xie, Z.; Xu, S.; Su, Y.; Yao, X.; Beyerlein, I.J. Effects of lattice distortion and chemical short-range order on the mechanisms of deformation in medium entropy alloy CoCrNi. *Acta Mater.* **2020**, *199*, 352–369. [CrossRef]
3. Gludovatz, B.; Hohenwarter, A.; Catoor, D.; Chang, E.H.; George, E.P.; Ritchie, R.O. A fracture-resistant high-entropy alloy for cryogenic applications. *Science* **2014**, *345*, 1153–1158. [CrossRef]
4. Gludovatz, B.; Hohenwarter, A.; Thurston, K.V.S.; Bei, H.; Wu, Z.; George, E.P.; Ritchie, R.O. Exceptional damage-tolerance of a medium-entropy alloy CrCoNi at cryogenic temperatures. *Nat. Commun.* **2016**, *7*, 10602. [CrossRef] [PubMed]
5. Laplanche, G.; Kostka, A.; Reinhart, C.; Hunfeld, J.; Eggeler, G.; George, E.P. Reasons for the superior mechanical properties of medium-entropy CrCoNi compared to high-entropy CrMnFeCoNi. *Acta Mater.* **2017**, *128*, 292–303. [CrossRef]
6. Liu, S.F.; Wu, Y.; Wang, H.T.; He, J.Y.; Liu, J.B.; Chen, C.X.; Liu, X.J.; Wang, H.; Lu, Z.P. Stacking fault energy of face-centered-cubic high entropy alloys. *Intermetallics* **2018**, *93*, 269–273. [CrossRef]
7. Woo, W.; Naeem, M.; Jeong, J.-S.; Lee, C.-M.; Harjo, S.; Kawasaki, T.; He, H.; Wang, X.-L. Comparison of dislocation density, twin fault probability, and stacking fault energy between CrCoNi and CrCoNiFe medium entropy alloys deformed at 293 and 140K. *Mater. Sci. Eng. A* **2020**, *781*, 139224. [CrossRef]
8. Cao, Y.Z.; Zhao, X.S.; Tu, W.D.; Yan, Y.D.; Yu, F.L. Plastic deformation mechanisms in face-centered cubic materials with low stacking fault energy. *Mater. Sci. Eng. A* **2016**, *676*, 241–245. [CrossRef]
9. Li, L.; Chen, H.; Fang, Q.; Li, J.; Liu, F.; Liu, Y.; Liaw, P.K. Effects of temperature and strain rate on plastic deformation mechanisms of nanocrystalline high-entropy alloys. *Intermetallics* **2020**, *120*, 106741. [CrossRef]
10. Utt, D.; Stukowski, A.; Able, K. Grain boundary structure and mobility in high-entropy alloys: A comparative molecular dynamics study on a Σ11 symmetrical tilt grain boundary in face-centered cubic CuNiCoFe. *Acta Mater.* **2020**, *186*, 11–19. [CrossRef]
11. Li, J.; Fang, Q.; Liu, B.; Liu, Y.; Liu, Y. Mechanical behaviors of AlCrFeCuNihigh-entropy alloys under uniaxial tension via molecular dynamics simulation. *RSC Adv.* **2016**, *6*, 76409–76419. [CrossRef]
12. Wang, Z.; Li, J.; Fang, Q.; Liu, B.; Zhang, L. Investigation into nanoscratchingmechanical response of AlCrCuFeNi high-entropy alloys using atomic simulations. *Appl. Surf. Sci.* **2017**, *416*, 470–481. [CrossRef]
13. Hirel, P. Atomsk: A tool for manipulating and converting atomic data files. *Comput. Phys. Commun.* **2015**, *197*, 212–219. [CrossRef]
14. Plimpton, S. Fast Parallel Algorithms for Short-Range Molecular Dynamics. *J. Comput. Phys.* **1995**, *117*, 1–19. [CrossRef]
15. Li, Q.-J.; Sheng, H.; Ma, E. Strengthening in multi-principal element alloys with local-chemical-order roughened dislocation pathways. *Nat. Commun.* **2019**, *10*, 1–11. [CrossRef] [PubMed]
16. Stukowski, A. Visualization and analysis of atomistic simulation data with OVITO-the open visualization tool. *Model. Simul. Mater. Sci. Eng.* **2010**, *18*, 015012. [CrossRef]
17. Honeycutt, J.D.; Andersen, H.C. Molecular dynamics study of melting and freezing of small Lennard-Jones clusters. *J. Phys. Chem.* **1987**, *91*, 4950–4963. [CrossRef]
18. Stukowski, A. Structure identification methods for atomistic simulations of crystalline materials. *Model. Simul. Mater. Sci. Eng.* **2012**, *20*, 045021. [CrossRef]
19. Stukowski, A.; Bulatov, V.V.; Arsenlis, A. Automated identification and indexing of dislocations in crystal interfaces. *Model. Simul. Mater. Sci. Eng.* **2012**, *20*, 085007. [CrossRef]
20. Yan, S.; Zhou, H.; Xing, B.; Zhang, S.; Li, L.; Qin, Q.H. Crystal plasticity in fusion zone of a hybrid laser welded Al alloys joint: From nanoscale to macroscale. *Mater. Des.* **2018**, *160*, 313–324. [CrossRef]
21. Yan, S.; Xing, B.; Qin, Q.-H. Effect of Interface on the Deformation of Aluminium Bicrystal: Atomistic Simulation Study. *MATEC Web Conf.* **2016**, *82*, 02010. [CrossRef]
22. Liang, Y.; Yang, X.; Ming, K.; Xiang, S.; Liu, Q. In situ observation of transmission and reflection of dislocations at twin boundary in CoCrNi alloys. *Sci. China Technol. Sci.* **2021**, *64*, 407–413. [CrossRef]
23. Deng, H.W.; Xie, Z.M.; Zhao, B.L.; Wang, Y.K.; Wang, M.M.; Yang, J.F.; Zhang, T.; Xiong, Y.; Wang, X.P.; Fang, Q.F.; et al. Tailoring mechanical properties of a CoCrNi medium-entropy alloy by controlling nanotwin-HCP lamellae and annealing twins. *Mater. Sci. Eng.* **2019**, *744*, 241–246. [CrossRef]